Tussilagonone Ameliorates Psoriatic Features in Keratinocytes and Imiquimod-Induced Psoriasis-Like Lesions in Mice via NRF2 Activation

Joohee Lee[1,2], Kwangho Song[1], Paul Hiebert[3], Sabine Werner[3], Tae-Gyun Kim[2] and Yeong Shik Kim[1,4]

Psoriasis is a common inflammatory skin disorder that is characterized by keratinocyte hyperproliferation and abnormal differentiation, resulting in the thickening of the epidermis and stratum corneum. In this study, we investigated *in vitro* and *in vivo* pharmacological effects of tussilagonone (TGN), a sesquiterpenoid isolated from *Tussilago farfara*, on transcription factors relevant for the pathogenesis of psoriasis. TGN inhibited activation of NF-κB and STAT3, leading to the attenuated expression of psoriasis-related inflammatory genes and suppression of keratinocyte hyperproliferation. Mechanistically, we show that the inhibition of NF-κB and STAT3 by TGN is mediated through activation of the cytoprotective transcription factor NRF2. Evaluation of *in vivo* antipsoriatic effects of topical TGN in the imiquimod-induced psoriasis-like dermatitis mouse model demonstrated amelioration of imiquimod-induced phenotypical changes, lesion severity score, epidermal thickening, and reduction in dermal cellularity. The spleen index also diminished in TGN-treated mice, suggesting anti-inflammatory properties of TGN. Moreover, TGN significantly attenuated the imiquimod-induced mRNA levels of psoriasis-associated inflammatory cytokines and antimicrobial peptides and reduced epidermal hyperproliferation. Taken together, TGN, as a potent NRF2 activator, is a promising therapeutic candidate for the development of antipsoriatic agents derived from medicinal plants.

Journal of Investigative Dermatology (2020) **140,** 1223–1232; doi:10.1016/j.jid.2019.12.008

INTRODUCTION

Psoriasis is a chronic immune-mediated skin disease with a prevalence of 2–3% in the world's population. It is manifested as scaly plaques of red and thickened skin that results from epidermal hyperproliferation, hyperparakeratosis (retention of nuclei in the stratum corneum), acanthosis (thickened epidermis) with elongated rete ridges, and immune cell infiltration (Boehncke and Schön, 2015; Nestle et al., 2009). Although the underlying cellular and molecular pathogenesis of psoriasis is complex and not fully understood, many lines of current evidence suggest that this skin disorder is mediated by the cross-talk between epidermal keratinocytes and immune cells (Hawkes et al., 2017; Lowes et al., 2014).

The dysregulated T helper type 17 pathway, including the IL-23/IL-17 axis, has been demonstrated as playing a key role in the immunopathogenesis of psoriasis (Cai et al., 2012; Hawkes et al., 2017; Martin et al., 2013). External stimuli, such as stress, trauma, infection, and drugs, and damage-associated molecular patterns can activate inflammatory and resident myeloid dendritic cells and macrophages to produce IL-23, IL-1β, and other proinflammatory cytokines including IL-6 and tumor necrosis factor-α (TNF-α). These innate immunity mediators stimulate the activities of key T-cell populations, such as T helper type 1, T helper type 17, and T helper type 22 cells, which release additional cytokines and chemokines. The proinflammatory cytokines and chemokines act on keratinocytes to induce hyperproliferation and impaired differentiation, leading to the development of psoriatic lesions (Greb et al., 2016; Martin et al., 2013; Muromoto et al., 2016). Psoriatic keratinocytes express inflammatory mediators including cytokines (IL-6, IL-1β, TNF-α, and granulocyte–macrophage colony-stimulating factor), chemokines (CXCL1, CXCL2, CCL20, and CXCL8), and antimicrobial peptides (S100A proteins and β-defensin). These mediators contribute to the activation of immune cells and feed back into the proinflammatory disease cycle, inducing psoriatic keratinocyte phenotypes and infiltration of dermal immune cells (Lowes et al., 2013).

Skin is the major target of oxidative stress, as it is continuously exposed to exogenous stressors, such as UV radiation, and endogenous stresses, such as skin metabolism and chronic inflammation, that induce the production of reactive oxygen species. Continued reactive oxygen species production may result in excessive oxidative stress, which contributes to many skin diseases including psoriasis (Ben-Yehuda Greenwald et al., 2016). Thus, an efficient antioxidative strategy that stimulates endogenous defense mechanisms is important for the treatment of psoriasis. The activation of the transcription factor NRF2 by several compounds was demonstrated to be

[1]*Natural Products Research Institute, College of Pharmacy, Seoul National University, Seoul, South Korea;* [2]*Department of Microbiology and Immunology, Department of Dermatology, Severance Hospital, Yonsei University College of Medicine, Seoul, South Korea;* [3]*Institute of Molecular Health Sciences, Department of Biology, Swiss Federal Institute of Technology (ETH) Zurich, Zurich, Switzerland; and* [4]*CHD Medics Co, Goyang, Gyeonggi, South Korea*

Correspondence: Yeong Shik Kim, College of Pharmacy, Seoul National University, 1 Gwanak-ro, Gwanak-gu, Seoul 08826, South Korea. E-mail: kims@snu.ac.kr

Abbreviations: ARE, antioxidant response element; CAL, calcipotriol; IMQ, imiquimod; TGN, tussilagonone; TNF-α, tumor necrosis factor-α

Received 3 May 2019; revised 2 December 2019; accepted 3 December 2019; accepted manuscript published online 23 December 2019; corrected proof published online 17 January 2020

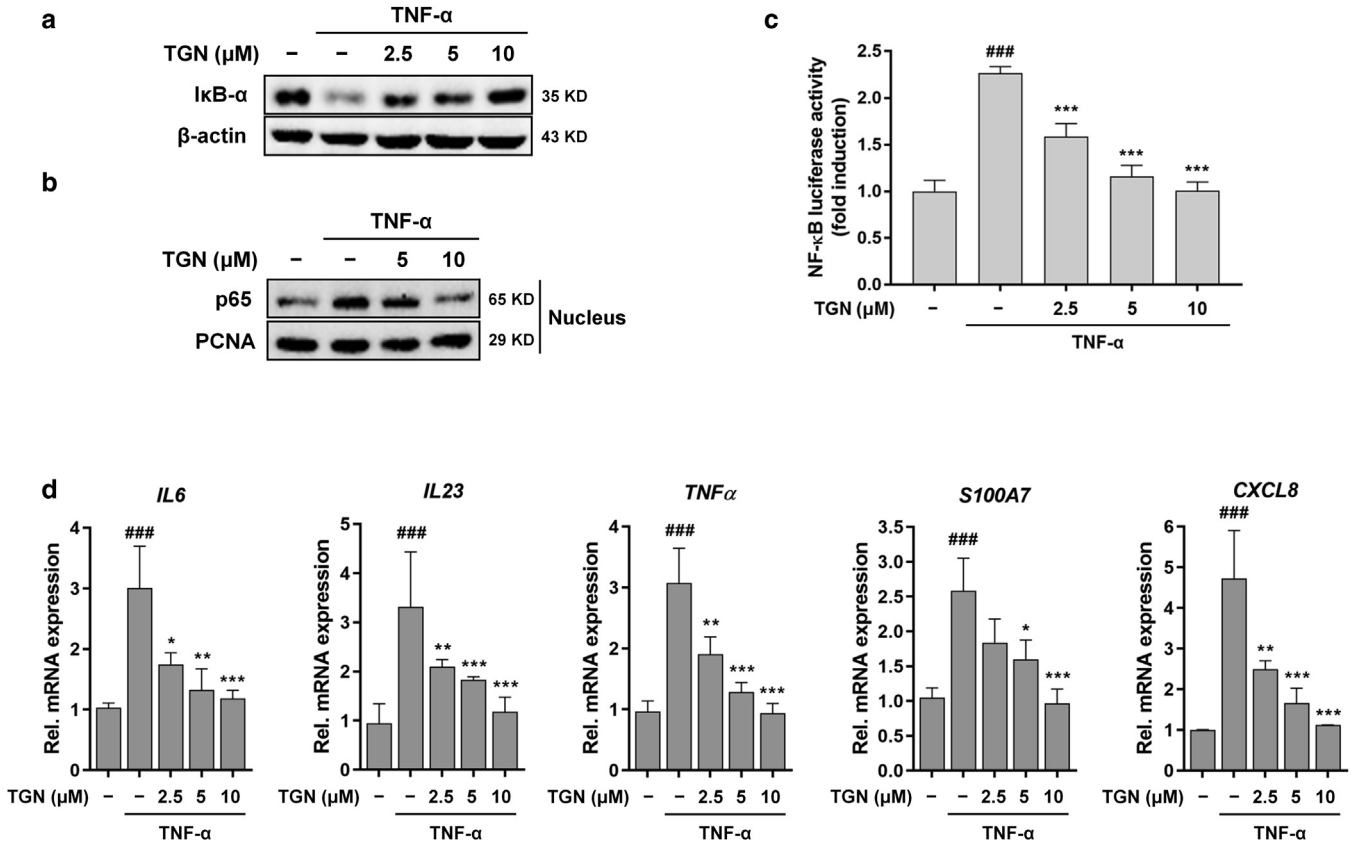

Figure 1. Inhibitory effects of TGN on TNF-α-induced NF-κB activation and mRNA expression of inflammatory mediators. (**a, b**) HaCaT cells were pretreated with TGN for 1 hour and then exposed to TNF-α for an additional 30 minutes. (a) Total or (b) nuclear protein lysates were used to determine the protein expression by western blot (n = 3). (**c**) HaCaT cells were pretreated with TGN for 1 hour and then with TNF-α for an additional 24 hours. NF-κB–luciferase activity was performed using a dual luciferase assay (n = 4). (**d**) HEKas were preincubated with TGN for 1 hour and then treated with TNF-α for an additional 6 hours. The mRNA levels were analyzed by real-time PCR (n = 6). $^{###}P < 0.001$ versus control. $^{**}P < 0.01$, $^{***}P < 0.001$ versus TNF-α group. HEKa, adult human epidermal keratinocyte; TGN, tussilagonone; TNF-α, tumor necrosis factor-α.

beneficial in the prevention of skin carcinogenesis in a variety of animal studies (Schäfer and Werner, 2015). In addition, NRF2 activation was also investigated as a promising treatment strategy for allergic skin inflammation, atopic dermatitis, psoriasis, epidermal blistering disease, and vitiligo vulgaris (reviewed by Schäfer and Werner, 2015).

Although there are some effective biological agents for the treatment of psoriasis that target proinflammatory cytokines, they are expensive and psoriasis usually relapses after treatment discontinuation for various reasons (Bellinato et al., 2019; Gottlieb, 2005). Therefore, the combination of biologics with other therapy can be synergistic with cost and dosage reduction for the treatment of psoriasis (Huang et al., 2019). We previously reported that tussilagonone (TGN), a sesquiterpenoid isolated from the buds of *Tussilago farfara*, exerts HO-1–mediated anti-inflammatory effects in macrophages and inhibitory effects on 12-*O*-tetradecanoylphorbol-13-acetate–induced acute skin inflammation in mice (Lee et al., 2016). Based on the previous study, it was hypothesized that TGN might be effective in other chronic inflammatory diseases, such as psoriasis, and that this effect could be mediated through activation of the NRF2 pathway.

The main objectives of this study were to (i) examine the therapeutic effect of TGN on psoriasis both *in vitro* and *in vivo* and (ii) characterize the cross-talk between NRF2, NF-κB, and STAT3 in psoriasis. To test the hypothesis of this study, the role of NRF2 activation by TGN in regulating STAT3 and NF-κB activation in keratinocytes was examined. Additionally, an optimal mouse model for chronic psoriatic skin inflammation was established, and the therapeutic potential of TGN against psoriasis was elucidated.

RESULTS

TGN inhibits TNF-α–induced NF-κB activation and the expression of psoriasis-related proinflammatory genes in keratinocytes

NF-κB is a transcription factor that regulates immune and inflammatory responses in various diseases, including psoriasis (Goldminz et al., 2013). To identify whether TGN can modulate TNF-α–induced NF-κB activation in human HaCaT keratinocytes, IκB-α degradation, as well as nuclear translocation of p65, one of the major subunits of NF-κB, was determined by western blot. Both TNF-α–induced IκB-α degradation and nuclear accumulation of p65 were inhibited by TGN in a dose-dependent manner (Figure 1a and b). Luciferase assay revealed that TGN pretreatment decreased NF-κB promoter activation by a TNF-α challenge (Figure 1c). We next examined whether TGN inhibited gene expression of proinflammatory cytokines involved in psoriasis using adult

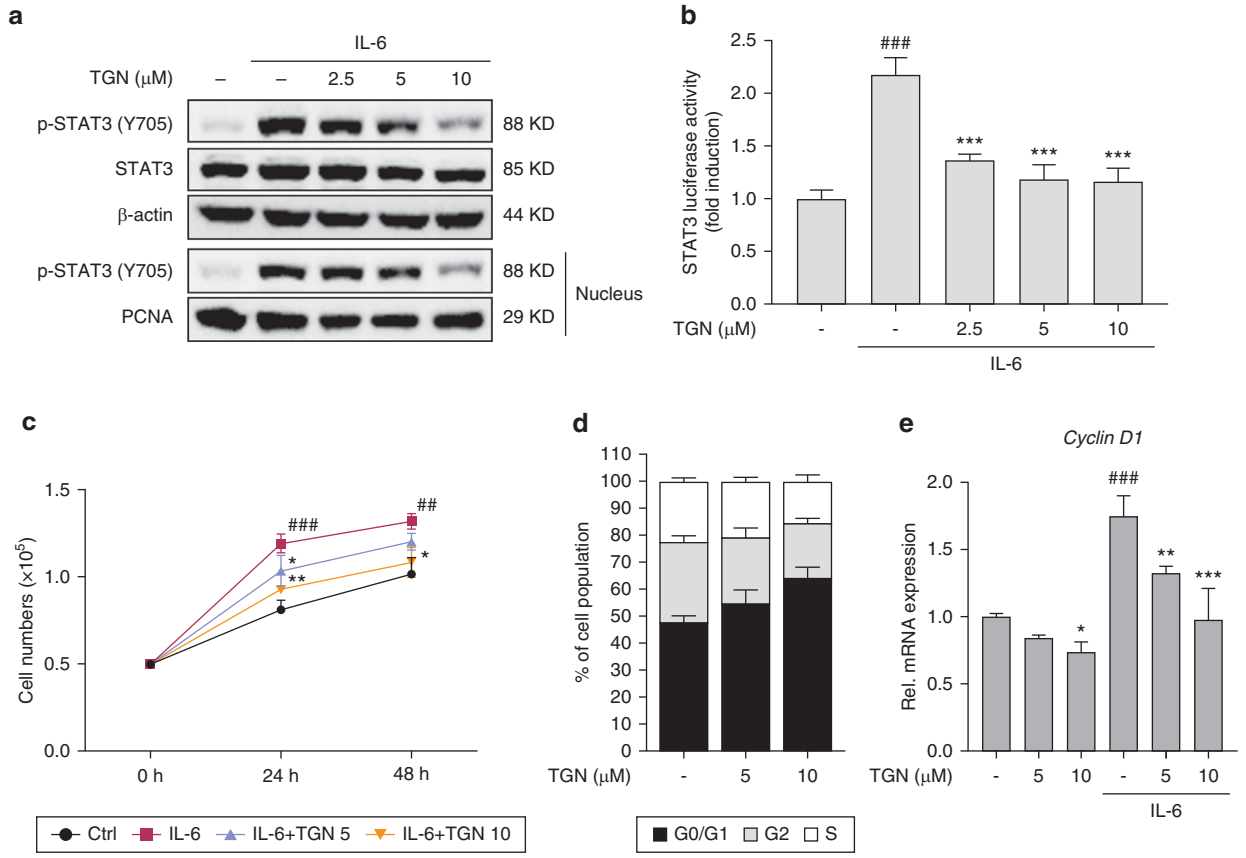

Figure 2. Inhibitory effects of TGN on IL-6–induced STAT3 activation and hyperproliferation. (**a**) HaCaT cells were stimulated with 25 ng/ml IL-6 for 30 minutes after TGN pretreatment. The phosphorylated STAT3 levels were detected by western blot (n = 3). (**b**) The HaCaT cells transfected with an NF-κB–regulated luciferase reporter construct were treated with IL-6 for 24 hours in the presence of TGN. The luciferase activity was measured (n = 4). (**c**) The number of HEKas were counted by trypan blue exclusion assay (n = 6). (**d**) Flow cytometric analysis of cell cycle with PI (n = 3). (**e**) HEKas were treated with IL-6 for 24 hours. The mRNA expression was analyzed by real-time PCR ($n = 6$). $^{###}P < 0.001$ versus control. $^{*}P < 0.05$, $^{**}P < 0.01$, and $^{***}P < 0.001$ versus IL-6 group. Ctrl, control; HEKa, adult human epidermal keratinocyte; PI, propidium iodide; TGN, tussilagonone.

human epidermal keratinocytes. TNF-α upregulated the relative mRNA levels of *IL-6*, *IL-23*, *TNF-α*, *S100A7*, and *CXCL8*, whereas pretreatment with TGN suppressed the mRNA levels of these cytokines (Figure 1d). Taken together, these results show that TGN inhibits TNF-α–induced inflammatory responses through impairment of NF-κB activation in keratinocytes.

TGN suppresses IL-6-induced STAT3 activation and keratinocyte proliferation

STAT3 is a therapeutic target for psoriasis as a key regulator involved in the regulation of cell proliferation and in the pathogenesis of psoriasis (Calautti et al., 2018; Sano et al., 2005). IL-6–induced phosphorylation and nuclear translocation of STAT3 were attenuated after treatment with TGN (Figure 2a). STAT3 luciferase activity was also reduced by TGN in a dose-dependent manner (Figure 2b). We further examined whether TGN inhibited proliferation of keratinocytes and the expression of proliferation markers. Adult human epidermal keratinocytes were stimulated with IL-6 in the presence or absence of TGN. TGN significantly inhibited IL-6–promoted cell proliferation (Figure 2c). Cell cycle analysis revealed that TGN treatment led to a G1/S growth arrest (Figure 2d) accompanied by decreased mRNA levels of G1-S progression regulator *Cyclin D1* (Figure 2e). These results indicate that TGN suppresses STAT3 activation leading to the inhibition of keratinocyte hyperproliferation.

TGN activates the NRF2/antioxidant response element (ARE) signaling pathway

NRF2 activation is considered as a promising therapeutic strategy in skin diseases, including psoriasis (Ben-Yehuda Greenwald et al., 2016; Schäfer and Werner, 2015). Our previous study has shown that TGN upregulates NRF2/HO-1 signaling in macrophages (Lee et al., 2016). Thus, we determined whether this regulatory action takes place in keratinocytes. TGN significantly promoted NRF2 and HO-1 protein expression and NRF2 nuclear localization in HaCaT keratinocytes (Figure 3a–c). To examine the effect of TGN on NRF2 transcriptional activity, a luciferase reporter gene assay was conducted. ARE-luciferase reporter activity reached a maximum level after 24 hours (Supplementary Figure S1) and increased dose-dependently at this time point (Figure 3d). Furthermore, the mRNA levels of *Ho1* and *Nqo1*, major target genes of NRF2, dramatically increased after TGN treatment for 24 hours in murine primary keratinocytes (Figure 3e). Sulforaphane and *tert*-butylhydroquinone, well known NRF2 activators, were used as positive controls. We next

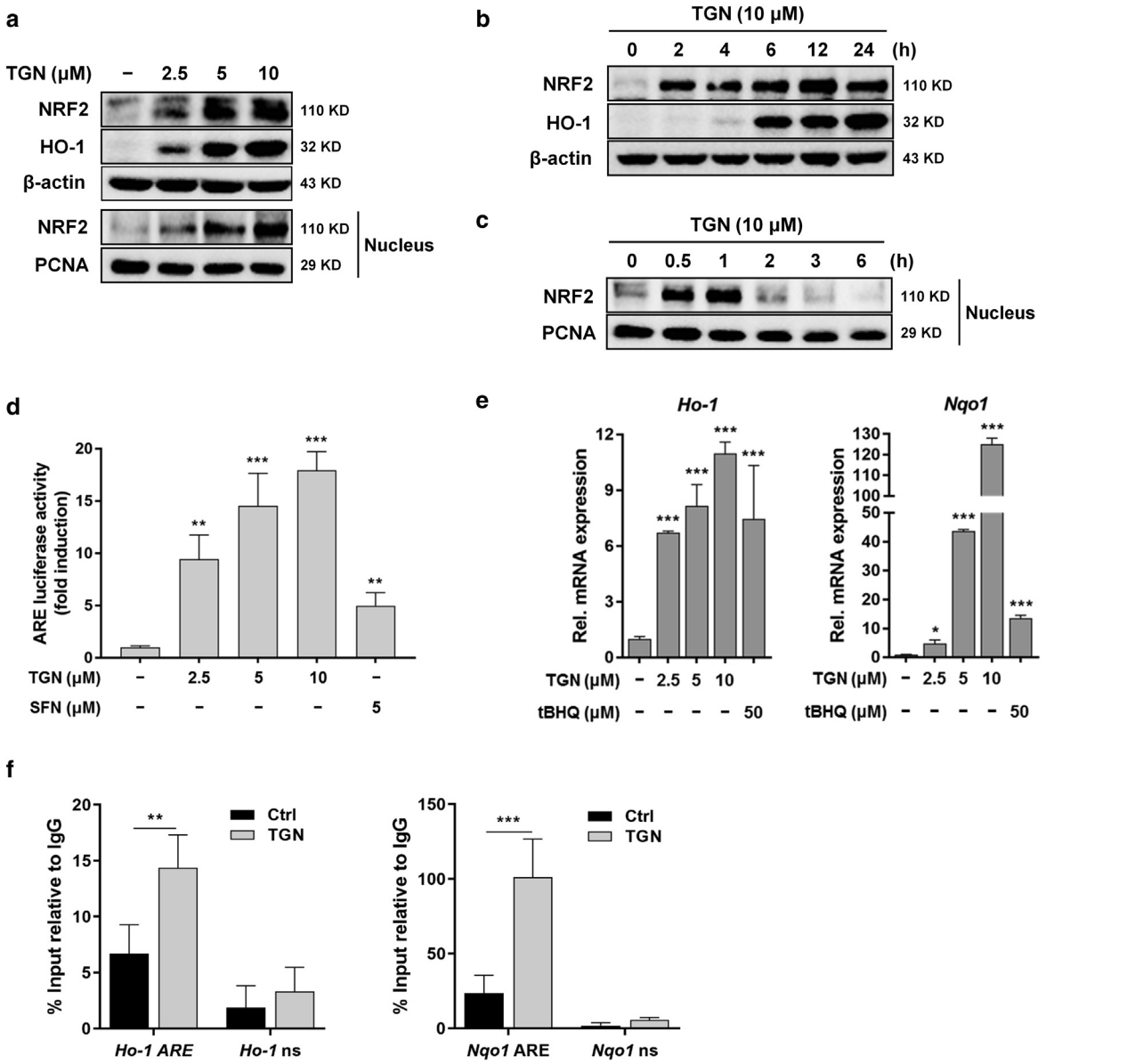

Figure 3. Effects of TGN on the activation of NRF2. (**a**–**c**) HaCaT cells were treated with (a) the indicated concentrations of TGN and (b, c) for the indicated times. Protein levels of NRF2 and HO-1 were determined by western blotting. (**d**) HaCaT cells were exposed to TGN for 24 hours and then ARE-luciferase activity was measured. (**e, f**) Primary murine keratinocytes were incubated with 10 μM TGN for 24 hours and then (e) mRNA levels were analyzed by real-time PCR or (f) a ChIP assay was conducted to assess binding of NRF2 to the ARE in the promoters of the genes encoding *Nqo1* and *Ho1*. The results shown are the mean ± SD of three experiments. *$P < 0.05$, **$P < 0.01$, and *** $P < 0.001$ versus control. ARE, antioxidant response element; ChIP, chromatin immunoprecipitation; SD, standard deviation; tBHQ, *tert*-butylhydroquinone; TGN, tussilagonone.

performed the chromatin immunoprecipitation assay to verify whether NRF2, which translocates into the nucleus, directly binds to the ARE in the *Ho1* and *Nqo1* promoter regions. Results showed that NRF2 was abundantly bound to the ARE sequences of the *Ho1* and *Nqo1* genes in primary mouse keratinocytes treated with TGN for 24 hours compared with the nontreated control cells. (Figure 3f). There were no significant differences between the control (nontreated) and the TGN-treated groups for binding to a nonspecific control region. Overall, these findings suggest that TGN activates the NRF2 signaling pathway through direct NRF2 binding to AREs present in the promoter or enhancer regions of NRF2 target genes and their subsequent transcription.

Inhibition of NF-κB and STAT3 by TGN is mediated through NRF2 activation

To investigate a potential effect of NRF2 on NF-κB and STAT3 activation, HaCaT cells were transfected with small interfering RNA or exposed to SnPP, a HO-1-specific inhibitor. The knockdown of NRF2 or HO-1 by small interfering RNA and inhibition of HO-1 activity by SnPP abrogated TGN-mediated inhibition of IκB-α degradation (Figure 4a and b). Similarly, silencing NRF2 or HO-1 inhibition abolished the inhibitory effect of TGN on STAT3 phosphorylation (Figure 4c and d). These results indicate that NRF2 activation and subsequent expression of its target HO-1 by TGN can regulate cytokine-induced activation of NF-κB and STAT3 in keratinocytes.

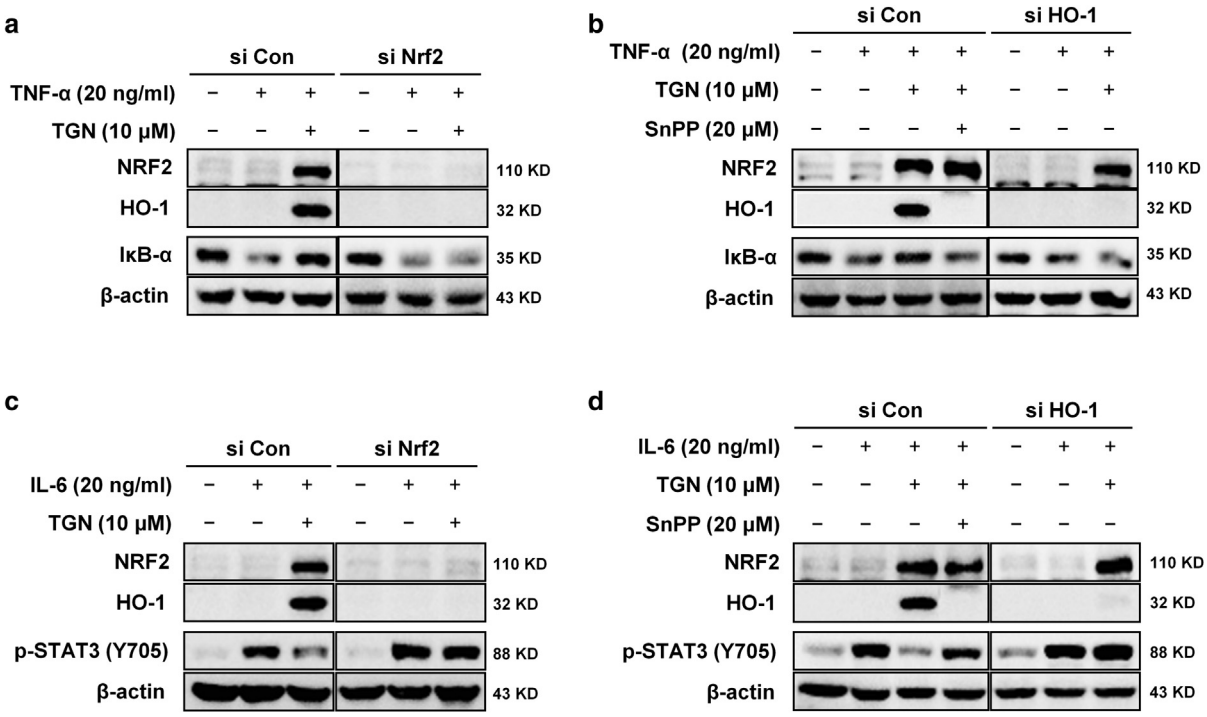

Figure 4. NRF2/HO-1 signaling-mediated inhibition of NF-κB and STAT3. (**a**–**d**) HaCaT cells were transfected with 50 nM of control siRNA (si Con), NRF2-targeting siRNA (si NRF2), or HO-1-targeting siRNA (si HO-1) for 48 hours and then incubated with (a, b) TNF-α or (c, d) IL-6 for 30 minutes after pretreatment with 10 μM of TGN for 6 hours. The results shown are representative of three independent experiments. siRNA, small interfering RNA; TGN, tussilagonone; TNF-α, tumor necrosis factor-α.

Topical TGN treatment ameliorates imiquimod (IMQ)-induced psoriasis-like skin inflammation in mice

As topical application of IMQ, a toll-like receptor 7/8 ligand and potent immune activator, on mouse skin mimics human psoriasis lesions (van der Fits et al., 2009), we evaluated potential *in vivo* antipsoriatic effects of TGN using the IMQ-induced psoriasis-like skin inflammation model in mice (Figure 5a). Mice were topically treated with 5% IMQ cream or control Vaseline cream on the shaved back skin and right ear for the first five consecutive days and were then cotreated with 1 or 5 nmol/100 μl of TGN and IMQ, respectively, for a further nine days (Figure 5a). Calcipotriol (CAL) was used as a positive control. On the fifth day, the IMQ-treated mice showed a remarkably thickened, erythematous, and scaly back skin compared with the control group mice, reflecting psoriasis-like skin condition (Figure 5c and Supplementary Figure S2). Phenotypical changes of the back skin and right ear (Figure 5b) and lesion severity score (Figure 5c and d) showed that topical treatment of TGN considerably attenuated IMQ-induced psoriatic traits. The spleen index (spleen weight to body weight ratio) also diminished in TGN-treated mice compared with mice treated with IMQ alone, suggesting the anti-inflammatory property of TGN (Figure 5e and f).

TGN reduces expression of inflammatory genes and epidermal hyperproliferation in IMQ-induced psoriasis-like mouse skin

To further confirm the antipsoriatic efficacy of topical TGN treatment, skin tissues obtained from mice after 14 days of topical treatment with IMQ were analyzed. Histopathological analysis of back skin and ear sections with using hematoxylin and eosin staining showed a reduction of IMQ-induced epidermal thickening (acanthosis) and dermal infiltrating cells in TGN-treated skin (Figure 6a–c). The expression of NF-κB p65 assessed by immunochemistry staining was increased by IMQ treatment, whereas TGN treatment almost completely inhibited the IMQ-induced p65 expression (Figure 6d). Moreover, TGN application significantly attenuated the IMQ-induced mRNA levels of psoriasis-associated inflammatory cytokines (*Il17a*, *Il22*, *Il23a*, and *Tnfa*) as well as antimicrobial peptides (*S100a7*, *S100a8*, *S100a9*, and *Defb4*) in skin (Figure 6e and f). Analysis of keratinocyte proliferation showed reduced numbers of Ki-67–positive cells in the epidermis of TGN-treated mice compared with mice treated with IMQ alone (Figure 6g). Furthermore, western blot analysis of total skin lysates revealed that IMQ-stimulated STAT3 phosphorylation was inhibited after topical treatment with TGN (Figure 6h). Taken together, these results support that TGN ameliorated IMQ-induced psoriasis-like skin lesions *in vivo* through inhibition of NF-κB and STAT3 and psoriasis-associated markers.

DISCUSSION

This study was designed to investigate whether TGN, which showed anti-inflammatory effects and activated the NRF2/HO-1 signaling pathway in a previous study performed with macrophages (Lee et al., 2016), alleviates psoriatic features in keratinocytes *in vitro* and in an IMQ-induced psoriasis-like dermatitis model in mice. We show that TGN attenuated cytokine-induced psoriatic activation of NF-κB and STAT3, which are crucial transcription factors involved in the

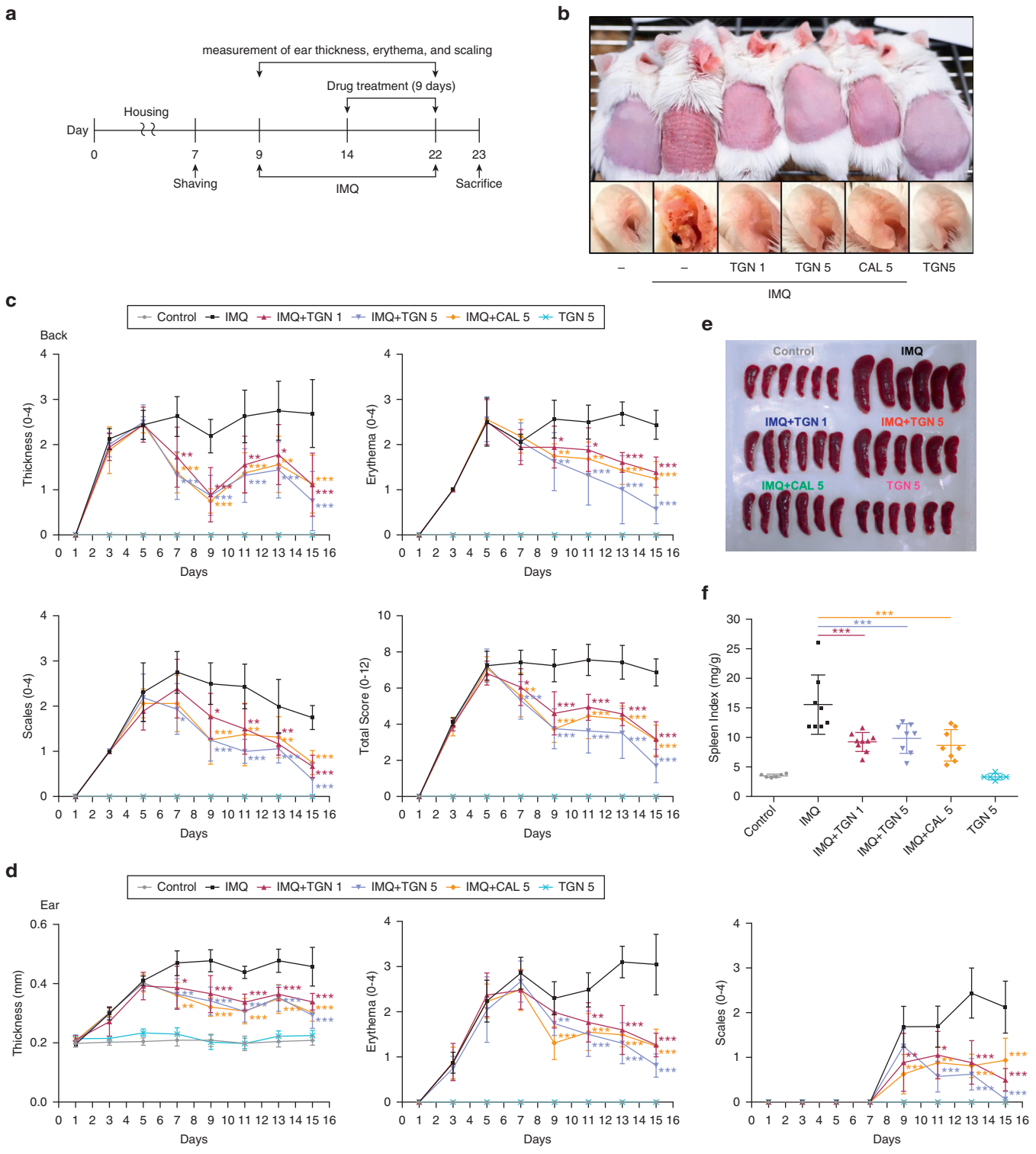

Figure 5. Effects of topical TGN on IMQ-induced psoriasis-like dermatitis in a mouse model. (**a**) Experimental scheme. (**b**) Macroscopic presentation of mice on the 15th day after IMQ treatment. (**c**) Quantitative severity assessment throughout the 14-day experimental period (n = 6–9). Thickness, erythema, and scaling of the back skin were scored every other day on a scale from 0 to 4. The cumulative score was calculated and presented as the mean ± SD. $^{*}P < 0.05$, $^{**}P < 0.01$, and $^{***}P < 0.001$ versus IMQ-treated group. (**d**) Thickness of the right ear was measured with a caliper, and erythema and scaling were scored every other day. (**e**) Representative morphology of spleens of each group. (**f**) Spleen index (spleen weight/body weight) was calculated (n = 6–9). $^{***}P < 0.001$ versus IMQ-treated group. CAL, calcipotriol; IMQ, imiquimod; TGN, tussilagonone.

pathogenesis of psoriasis. Furthermore, the activation of NRF2/HO-1 by TGN-mediated NF-κB and STAT3 inhibition (Supplementary Figure S3). Topical administration of TGN exerted inhibitory effects on IMQ-induced psoriatic skin lesions, highlighting the potential for TGN as an antipsoriatic agent.

The pathophysiology of psoriasis is multifactorial, which is associated with a number of biochemical and immunological disturbances. It has been demonstrated that oxidative stress is involved in the pathogenesis of psoriasis (Kadam et al., 2010). Dimethylfumarate, the main ingredient of oral fumaric acid esters (Fumaderm), which has been used as a systemic therapy for the treatment of moderate to severe forms of psoriasis, is a potent NRF2 activator through its capacity to directly modulate specific cysteine residues in the NRF2 antagonist KEAP1 (Brennan et al., 2015). Preclinical studies have demonstrated that dimethylfumarate exhibits anti-inflammatory and cytoprotective activities that are partially mediated by the NRF2 antioxidant response pathway (Fox et al., 2014). Additionally, several studies revealed that pharmacological upregulation of HO-1 contributes to the attenuation of psoriatic features *in vitro* and *in vivo* (An et al., 2016; Campbell et al., 2018; Zhang et al., 2016). TGN significantly activated NRF2 and induced expression of its downstream target gene *HO1/Ho1* in keratinocytes. Activation of NRF2/HO-1 by TGN suppressed the activation of NF-κB and STAT3, resulting in the suppression of inflammatory responses and keratinocyte hyperplasia, the main features of psoriatic lesions. The present results demonstrate that NRF2 activation by TGN might be used therapeutically for the treatment of psoriasis by modulating the activation of transcription factors associated with psoriasis as well as by promoting the defense system of the skin.

The IMQ-induced murine model is widely used to study psoriasis-like skin dermatitis in mice. IMQ is a ligand for TLR7 and TLR8 and a potent immune activator. Topical application of IMQ produces psoriasis-like skin lesions in mice, which display many of the same phenotypic and histological characteristics as those observed in psoriasis in humans: induction of acanthosis, parakeratosis, and a mixed inflammatory infiltrate mediated by elevation of the IL-23/IL-17 axis (van der Fits et al., 2009). It was also shown that the application of IMQ on human nonlesional psoriatic skin resulted in psoriasis-like skin inflammation, although it differs somewhat from typical psoriasis in patients (Vinter et al., 2015). In this study, IMQ was topically applied to the mouse's back skin and right ear for five consecutive days. On the fifth day of IMQ treatment, psoriasis-like skin conditions were observed, such as increased skin thickness and increased lesion severity score for erythema and scaling in the IMQ group compared with the control group. Cotreatment with IMQ and TGN for nine more days ameliorated both phenotypical and histological changes of psoriasis induced by IMQ. In addition, TGN inhibited NF-κB and STAT3 activation and reduced the expression of immune mediators and epidermal proliferation in skin tissue homogenates. These results are in consistent with the findings of the *in vitro* studies.

The spleen is the largest secondary lymphoid organ in the immune system, and its enlargement with an increase in weight represents the increase of cells in the spleen and the elevation of immune reactions (Qin et al., 2014; van der Fits et al., 2009). Topical administration of TGN significantly reduced the IMQ-induced spleen index, indicating an anti-inflammatory effect of TGN. Because TGN exerts therapeutic effects on psoriatic lesions through the modulation of psoriasis-associated transcription factors, it can be seen as a result of a systematic immune response. Further studies are required to determine how topical treatment of TGN directly or indirectly affects the immune system and clarify the pharmacokinetic profile of TGN after topical application.

Vitamin D analogs, such as CAL, tacalcitol, and maxacalcitol, are the most popularly prescribed first-line topical treatments for psoriasis (Barrea et al., 2017). The biological activities of vitamin D analogs are mediated through the vitamin D receptor, a ligand-activated transcription factor, which regulates gene transcription in target cells such as keratinocytes and lymphocytes (Carlberg and Campbell, 2013). A recent study demonstrated that topical CAL application exerted an antipsoriatic effect in a murine model of psoriasis by controlling the IL-23/IL-17A axis and systemic burden of pathogenic T17 cells (Kusuba et al., 2018). Here, topical treatment of TGN in mice showed comparable effects to CAL by regulating transcription factors involved in the pathogenesis of psoriasis. We found that TGN, but not CAL, induced activation of NRF2/HO-1, showing that TGN and CAL have a different mechanism of action (Figure 3a and Supplementary Figure S4). In addition, CAL-mediated inactivation of STAT3 in IMQ-treated skin (Figure 6h) seems to be an indirect response accompanied by the suppression of the IL-23/IL-17 axis (Germán et al., 2019; Kusuba et al., 2018). Several studies have indicated that CAL can induce significant ear swelling and atopic dermatitis-like skin inflammation (Kim et al., 2013; Li et al., 2006). The most common side effect of CAL is skin irritation (red, dry, and itchy skin), exhibiting similarities with atopic dermatitis lesions (Gottlieb, 2005). If further studies reveal that TGN has fewer side effects than CAL, TGN could be useful as a safe topical treatment for psoriasis.

In conclusion, it was demonstrated that TGN diminishes the activation of NF-κB and STAT3 in keratinocytes *in vitro* and in mice. A TGN-activated NRF2 pathway has an essential role in the regulation of these transcription factors. Thus, pharmacological NRF2 activation may relieve psoriasis symptoms through the signaling cross-talk with psoriasis-related transcription factors. Furthermore, in an IMQ-induced psoriasis-like dermatitis mouse model, topical TGN treatment not only provided local symptomatic benefit but also contributed to the control of systemic immune responses. Taken together, TGN, a naturally derived compound that can activate NRF2, will be of interest for the development of a new drug for psoriasis.

MATERIALS AND METHODS

Experimental details are described in Supplementary Materials and Methods.

Cell culture

Human HaCaT cells were originally obtained from Dr Norbert E. Fusenig (German Cancer Research Center, Heidelberg, Germany) and subcultured in our laboratory. The cells were cultured in DMEM supplemented with 10% fetal bovine serum, 100 U/ml penicillin, and 100 μg/ml streptomycin. Adult human epidermal keratinocytes (Gibco, Life Technologies, Carlsbad, CA) were cultured in EpiLife Medium supplemented with Human Keratinocyte Growth

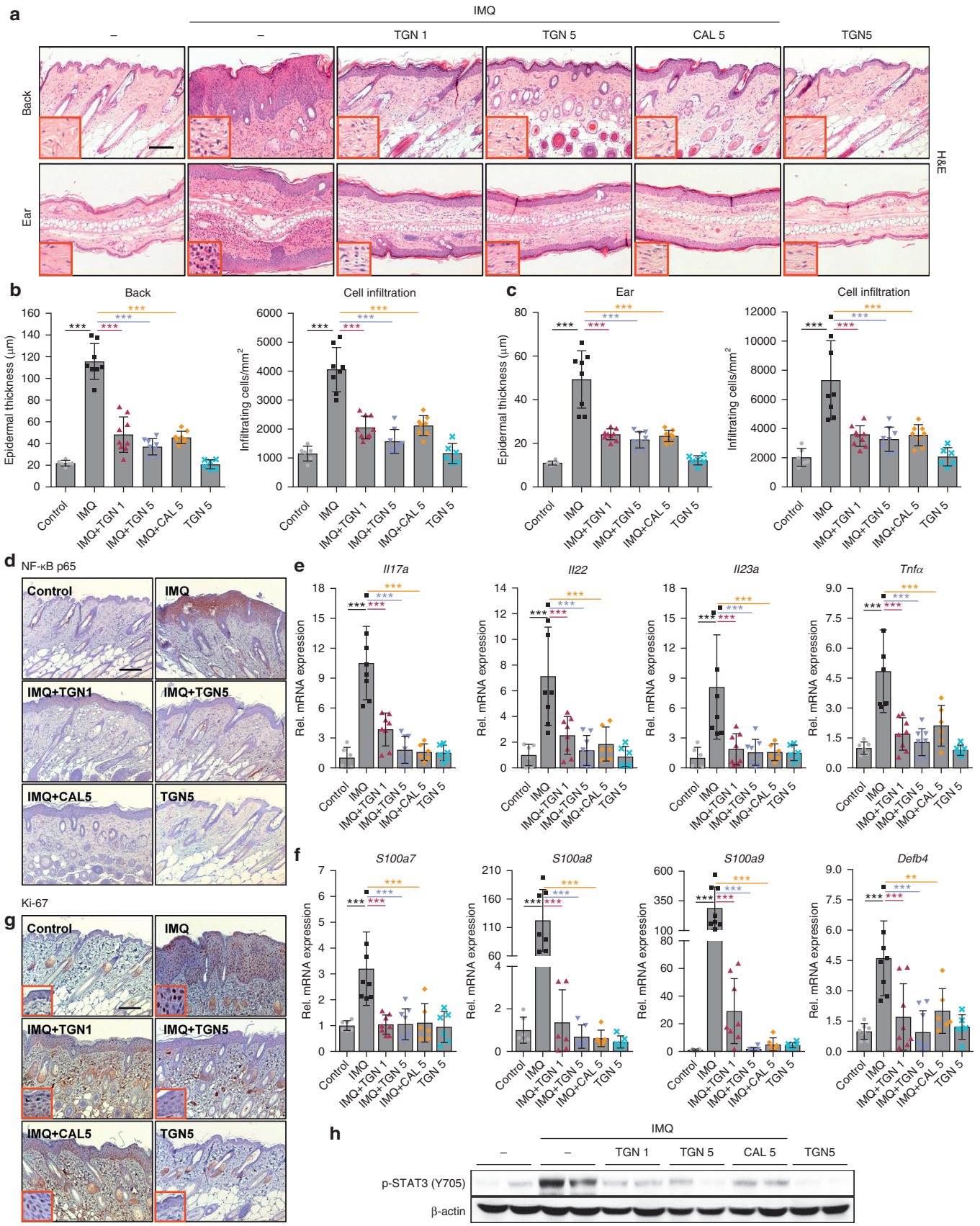

Figure 6. Inhibitory effects of TGN on the expression of inflammatory genes and epidermal hyperproliferation in IMQ-induced psoriasis-like mouse skin. (**a**) H&E staining of skin biopsies (magnification, ×200). Insets with red box show increased immune cell influx (magnification, ×400). Bar = 100 μm. (**b, c**) Epidermal thickness and number of infiltrating cells of the (b) back and (c) ear skin in representative HPFs (n = 6–9). (**d**) Immunohistochemical analysis of NF-κB p65 in the epidermis (magnification, ×200). Bar = 100 μm. (**e, f**) mRNA from back skin of Balb/c mice was analyzed for expression of (e) inflammatory cytokines

Supplement (Gibco, Life Technologies). Cells were maintained at 37°C in a humidified atmosphere of 5% CO_2 and 95% air.

Animals

Female Balb/c mice (7 weeks old, 17−20 g) were purchased from Koatech Co (Pyeongtaek, Korea). All mice were housed in a pathogen-free barrier zone of the Seoul National University Animal Laboratory at 22 ± 2°C with 50 ± 5% humidity in a 12-hour light/dark cycle. All animal studies were performed according to the approved guidelines of Seoul National University Institutional Animal Care and Use Committees (approval ID: SNU-180206-1).

IMQ-induced psoriasis-like dermatitis model in mice

The back skin of the mice was shaved using an electric clipper and then treated with a depilatory cream to remove residual hairs 2 days before treatment. The mice were divided into the following six groups, with 6−9 mice for each group: (i) Vehicle control group (Vaseline cream plus ethanol-treated group), (ii) IMQ group (IMQ plus ethanol-treated group); (iii) IMQ + TGN 1 nmol/100 μl group (IMQ plus TGN 1 nmol-treated group); (iv) IMQ + TGN 5 nmol/100 μl group (IMQ plus TGN 5 nmol-treated group); (v) IMQ + CAL 5 nmol/100 μl group (IMQ plus CAL 5 nmol-treated group); and (vi) TGN 5 nmol/100 μl group (Vaseline cream plus TGN 5 nmol-treated group). Whereas control mice received a control cream, the IMQ-treated mice received a daily topical dose of 20 and 62.5 mg of 5% IMQ cream (Aldara, 3M Pharmaceuticals, Maplewood, MN) on the right ear and the shaved back skin, respectively, for five consecutive days to induce the disease before drug treatment. The IMQ group and IMQ + drug groups continued to receive the same dose of IMQ for a total of 14 consecutive days to achieve optimal chronic inflammation. From day 6, the IMQ + drug groups first received topical application of TGN or CAL. The back and ear skin were topically treated with TGN or CAL dissolved in ethanol in a volume of 100 μl (on shaved back skin) or 20 μl (10 μl on each side of the right ear) daily from days 6−15.

Statistical analysis

The results represent the mean ± standard deviation from at least three different experiments. Statistical analyses were performed with a one-way analysis of variance with Dunnett's and/or Bonferroni's multiple comparisons test using GraphPad Prism 7.0 software (San Diego, CA). *P*-values less than 0.05 were considered statistically significant.

Data availability statement

The data analyzed during this study are included in this published article and its supplementary information file.

ORCIDs

Joohee Lee: http://orcid.org/0000-0003-3877-5752
Kwangho Song: http://orcid.org/0000-0002-1822-7137
Paul Hiebert: http://orcid.org/0000-0001-8179-4217
Sabine Werner: http://orcid.org/0000-0001-7397-8710
Tae-Gyun Kim: http://orcid.org/0000-0002-2116-4579
Yeong Shik Kim: http://orcid.org/0000-0003-1353-3925

CONFLICT OF INTEREST

The authors state no conflict of interest.

ACKNOWLEDGMENTS

This work was supported by grants from the National Research Foundation of Korea (NRF-2017R1A2B4009301, 2016K1A3A1A14953231, and 2019R1A6A1A03032869) and the Korea Institute of Science and Technology (KIST370C-20190043). Part of this study was conducted as a fellow in the "Young Researchers Exchange Program between Korea and Switzerland" under the "Korean-Swiss Science and Technology Program."

AUTHOR CONTRIBUTIONS

Conceptualization: JL, YSK; Data Curation: JL; Formal Analysis: JL, KS; Funding Acquisition: YSK; Investigation: JL, KS; Methodology: JL, KS, PH; Project Administration: PH, YSK; Resources: SW, YSK; Supervision: SW, YSK; Validation: JL, YSK; Visualization: JL; Writing - Original Draft Preparation: JL; Writing - Review and Editing: JL, SW, T-GK, YSK.

SUPPLEMENTARY MATERIAL

Supplementary material is linked to the online version of the paper at www.jidonline.org, and at https://doi.org/10.1016/j.jid.2019.12.008.

REFERENCES

An J, Li T, Dong Y, Li Z, Huo J. Terminalia Chebulanin attenuates psoriatic skin lesion via regulation of heme Oxygenase-1. Cell Physiol Biochem 2016;39:531−43.

Barrea L, Savanelli MC, Di Somma C, Napolitano M, Megna M, Colao A, et al. Vitamin D and its role in psoriasis: an overview of the dermatologist and nutritionist. Rev Endocr Metab Disord 2017;18:195−205.

Bellinato F, Girolomoni G, Gisondi P. Relapse of psoriasis in patients who asked to discontinue etanercept after achieving a stable clinical remission. Br J Dermatol 2019;181:1319−20.

Ben-Yehuda Greenwald M, Ben-Sasson S, Bianco-Peled H, Kohen R. Skin redox balance maintenance: the need for an Nrf2-activator delivery system. Cosmetics 2016;3:1.

Boehncke WH, Schön MP. Psoriasis. Lancet 2015;386:983−94.

Brennan MS, Matos MF, Li B, Hronowski X, Gao B, Juhasz P, et al. Dimethyl fumarate and monoethyl fumarate exhibit differential effects on KEAP1, NRF2 activation, and glutathione depletion in vitro. PLOS ONE 2015;10:e0120254.

Cai Y, Fleming C, Yan J. New insights of T cells in the pathogenesis of psoriasis. Cell Mol Immunol 2012;9:302−9.

Calautti E, Avalle L, Poli V. Psoriasis: a STAT3-centric view. Int J Mol Sci 2018;19:171.

Campbell NK, Fitzgerald HK, Malara A, Hambly R, Sweeney CM, Kirby B, et al. Naturally derived Heme-Oxygenase 1 inducers attenuate inflammatory responses in human dendritic cells and T cells: relevance for psoriasis treatment. Sci Rep 2018;8:10287.

Carlberg C, Campbell MJ. Vitamin D receptor signaling mechanisms: integrated actions of a well-defined transcription factor. Steroids 2013;78:127−36.

Fox RJ, Kita M, Cohan SL, Henson LJ, Zambrano J, Scannevin RH, et al. BG-12 (dimethyl fumarate): a review of mechanism of action, efficacy, and safety. Curr Med Res Opin 2014;30:251−62.

Germán B, Wei R, Hener P, Martins C, Ye T, Gottwick C, et al. Disrupting the IL-36 and IL-23/IL-17 loop underlies the efficacy of calcipotriol and corticosteroid therapy for psoriasis. JCI Insight 2019;4:e123390.

Goldminz AM, Au SC, Kim N, Gottlieb AB, Lizzul PF. NF-kappaB: an essential transcription factor in psoriasis. J Dermatol Sci 2013;69:89−94.

Gottlieb AB. Therapeutic options in the treatment of psoriasis and atopic dermatitis. J Am Acad Dermatol 2005;53:S3−16.

Gottlieb AB. Psoriasis: emerging therapeutic strategies. Nat Rev Drug Discov 2005;4:19−34.

Greb JE, Goldminz AM, Elder JT, Lebwohl MG, Gladman DD, Wu JJ, et al. Psoriasis. Nat Rev Dis Primers 2016;2:16082.

Hawkes JE, Chan TC, Krueger JG. Psoriasis pathogenesis and the development of novel targeted immune therapies. J Allergy Clin Immunol 2017;140:645−53.

and (f) antimicrobial peptides by qRT-PCR (n = 6−9). (**g**) Ki-67 immunohistochemical staining (magnification, ×200; red box, ×400). Bar = 100 μm. (**h**) STAT3 phosphorylation was detected by western blotting on protein extracts from back skin homogenates of mice. All samples were collected 24 hours after 14 applications of IMQ. CAL, calcipotriol; H&E, hematoxylin and eosin; HPF, high-power field; IMQ, imiquimod; qRT-PCR, quantitative real-time reverse transcriptase−PCR; TGN, tussilagonone.

Huang TH, Lin CF, Alalaiwe A, Yang SC, Fang JY. Apoptotic or anti-proliferative activity of natural products against keratinocytes for the treatment of psoriasis. Int J Mol Sci 2019;20:2558.

Kadam DP, Suryakar AN, Ankush RD, Kadam CY, Deshpande KH. Role of oxidative stress in various stages of psoriasis. Indian J Clin Biochem 2010;25:388–92.

Kim BS, Siracusa MC, Saenz SA, Noti M, Monticelli LA, Sonnenberg GF, et al. TSLP elicits IL-33–independent innate lymphoid cell responses to promote skin inflammation. Sci Transl Med 2013;5:170ra16.

Kusuba N, Kitoh A, Dainichi T, Honda T, Otsuka A, Egawa G, et al. Inhibition of IL-17–committed T cells in a murine psoriasis model by a vitamin D analogue. J Allergy Clin Immunol 2018;141:972–81.e10.

Lee J, Kang U, Seo EK, Kim YS. Heme oxygenase-1-mediated anti-inflammatory effects of tussilagonone on macrophages and 12-O-tetradecanoylphorbol-13-acetate-induced skin inflammation in mice. Int Immunopharmacol 2016;34:155–64.

Li M, Hener P, Zhang Z, Kato S, Metzger D, Chambon P. Topical vitamin D3 and low-calcemic analogs induce thymic stromal lymphopoietin in mouse keratinocytes and trigger an atopic dermatitis. Proc Natl Acad Sci USA 2006;103:11736–41.

Lowes MA, Russell CB, Martin DA, Towne JE, Krueger JG. The IL-23/T17 pathogenic axis in psoriasis is amplified by keratinocyte responses. Trends Immunol 2013;34:174–81.

Lowes MA, Suárez-Fariñas M, Krueger JG. Immunology of psoriasis. Annu Rev Immunol 2014;32:227–55.

Martin DA, Towne JE, Kricorian G, Klekotka P, Gudjonsson JE, Krueger JG, et al. The emerging role of IL-17 in the pathogenesis of psoriasis: preclinical and clinical findings. J Invest Dermatol 2013;133:17–26.

Muromoto R, Hirao T, Tawa K, Hirashima K, Kon S, Kitai Y, et al. IL-17A plays a central role in the expression of psoriasis signature genes through the induction of IkappaB-zeta in keratinocytes. Int Immunol 2016;28:443–52.

Nestle FO, Kaplan DH, Barker J. Psoriasis. N Engl J Med 2009;361:496–509.

Qin S, Wen J, Bai XC, Chen TY, Zheng RC, Zhou GB, et al. Endogenous n-3 polyunsaturated fatty acids protect against imiquimod-induced psoriasis-like inflammation via the IL-17/IL-23 axis. Mol Med Rep 2014;9:2097–104.

Sano S, Chan KS, Carbajal S, Clifford J, Peavey M, Kiguchi K, et al. Stat3 links activated keratinocytes and immunocytes required for development of psoriasis in a novel transgenic mouse model. Nat Med 2005;11:43–9.

Schäfer M, Werner S. Nrf2–A regulator of keratinocyte redox signaling. Free Radic Biol Med 2015;88:243–52.

van der Fits L, Mourits S, Voerman JS, Kant M, Boon L, Laman JD, et al. Imiquimod-induced psoriasis-like skin inflammation in mice is mediated via the IL-23/IL-17 axis. J Immunol 2009;182:5836–45.

Vinter H, Iversen L, Steiniche T, Kragballe K, Johansen C. Aldara®-induced skin inflammation: studies of patients with psoriasis. Br J Dermatol 2015;172:345–53.

Zhang B, Xie S, Su Z, Song S, Xu H, Chen G, et al. Heme oxygenase-1 induction attenuates imiquimod-induced psoriasiform inflammation by negative regulation of Stat3 signaling. Sci Rep 2016;6:21132.

SUPPLEMENTARY MATERIALS AND METHODS

Preparation of tussilagonone (TGN)

TGN was obtained by hydrolysis of tussilagone, which was preparatively separated from Farfarae Flos (Song et al., 2017). One gram of tussilagone was dissolved in 70% aqueous acetonitrile, and sodium hydroxide was added to the 100 mM solution. The reaction mixture was stirred at 25°C for 1 hour, followed by solvent extraction with chloroform. The lower layer (organic solvent) was evaporated and separated by counter-current chromatography. The conditions were as follows: n-hexane as stationary phase, water (eluent A) and acetonitrile (eluent B) as mobile phase, linear gradient, 0–100 min (70–90% B) and 100–150 min (90% B), at a flow rate of 8 ml/min and a rotation speed of 450 rpm. Eluate from 138–152 min was collected and dried (345 mg), followed by structural determination. The 1H and 13C NMR spectra were compared with previous literature (Park et al., 2008).

Isolation and culture of primary epidermal keratinocytes

Isolation and cultivation of murine primary keratinocytes was performed using newborn (from 2 to 4 days old) mice as previously described (Siegenthaler et al., 2018). Mice were immersed in 70% ethanol, then in sterile phosphate buffered saline, followed by 70% ethanol and, finally, again in phosphate buffered saline. Skin laid flat with the epidermis facing up was incubated in 2.5% trypsin at 37°C for 60 minutes, then the epidermis was separated from the dermis and incubated in DNase solution (0.25 mg/ml) for 20 minutes at 37°C while shaking at 80 rpm. The epidermis/DNase solution was then filtered through a 100-μm cell strainer and pelleted by centrifugation (1,200 rpm for 5 minutes). Cells were seeded on collagen-IV (2.5 g/cm^2)-coated dishes. The medium was changed the following day, and cells were grown to 90% confluency in defined keratinocyte medium (Invitrogen, Thermo Fisher Scientific, Waltham, MA), supplemented with 10 ng/ml epidermal growth factor and 10^{-10} M cholera toxin with low-calcium fetal bovine serum as done previously (Siegenthaler et al., 2018).

Western blot analysis

Total cell lysates and cytosolic and nuclear extracts were prepared as previously described (Lee et al., 2018). The protein concentration was quantified using the Bradford protein assay (Bio-Rad Laboratories, Hercules, CA). Equal amounts of protein (30 μg) were loaded on 8–10% of SDS–polyacrylamide gels and transferred to nitrocellulose membranes. The membranes were incubated with primary antibodies overnight at 4°C and incubated with horseradish peroxidase–conjugated secondary antibodies for 1 hour at room temperature. The immunoblots were detected with an EZ-Western detection kit (DoGEN, Seoul, Korea).

Quantitative real-time reverse transcriptase–PCR

RNA was isolated using the Trizol reagent kit (Invitrogen). One microgram of total RNA was synthesized into cDNA using the amfiRivert Platinum cDNA Synthesis Master Mix (GenDepot, Barker, TX) according to the manufacturer's instructions. PCR amplification of target genes was performed using forward and reverse primers and a SYBR Green working solution (iTaq Universal SYBR Green Supermix, Bio-Rad) with an Applied Biosystems 7300 real-time PCR system and software (Applied Biosystems, Carlsbad, CA). Gene expressions were normalized to *Gapdh* using the $2^{-\Delta\Delta Ct}$ method of relative quantification. The following primers were used: *h-GAPDH*, 5′-TGTTGCCATCAATGACCCCTT-3′ (F) and 5′-CTCCACGACGTACTCAGCG-3′ (F); *h-IL6*, 5′-AAATGC CAGCCTGCTGACGAAC-3′ (F) and 5′-AACAACAATCTG AGGTGCCCATGCTAC-3′ (R); *h-IL23*, 5′-CAGCAACCCT GAGTCCCTAA-3′ (F) and 5′-TCAACATATGCAGGTCCCACT -3′ (R); *TNFα*, 5′-TTCGTCTACTGAACTTCGGGGTGATCGG TCC-3′ (F) and 5′-GTATGAGATAGCAAATCGGCTGA CGGTGTGGG-3′ (R); *h-S100A7*, 5′-AGACGTGATGACAA GATTGAC-3′ (F) and 5′-TGTCCTTTTTCTCAAAGACGTC-3′ (R); *h-CXCL8*, 5′-GTCCTTGTTCCACTGTGCCT-3′ (F) and 5′-GCTTCCACATGTCCTCACAA-3′ (R); *m-Gapdh*, 5′-AGGTC GGTGTGAACGGATTTG-3′ (F) and 5′-GGGGTCGTTGA TGGCAACA-3′ (R); *m-Il17a*, 5′-CTCCAGAAGGCCCTCA GACTAC-3′ (F) and 5′-GGGTCTTCATTGCGGTGG-3′ (R); *m-Il22*, 5′-ATGAGTTTTTCCCTTATGGGGAC-3′ (F) and 5′-GCTGGAAGTTGGACACCTCAA-3′ (R); *m-Il23a*, 5′-AACTCC TCCAGCCAGAGGATCA-3′ (F) and 5′-TCTTGGAACGGA GAAGGGGG-3′ (R); *m-Tnfa*, 5′-TGCCTATGTCTCAGCC TCTTC-3′ (F) and 5′-GAGGCCATTTGGGAACTTCT-3′ (R); *m-S100a7*, 5′-GAGGAGTTGAAAGCTCTGCTCTTG-3′ (F) and 5′-GTGATGTAGTATGGCTGCCTGCGG-3′ (R); *m-S100a8*, 5′-AAATCACCATGCCCTCTACAAG-3′ (F) and 5′-CCCACTTTTATCACCATCGCAA-3′ (R); *m-S100a9*, 5′-GCA-CAGTTGGCAACCTTTATG-3′ (F) and 5′-TGATTGTCCTGGTT TGTGTCC-3′ (R); and *m-Defb4*, 5′-CTCCACTTGCAGCCTT TACC-3′ (F) and 5′-ATCTGTCGAAAAGCGGTAGGG-3′ (R).

Luciferase assay

HaCaT cells were cotransfected with 0.5 μg of pRL-CMV control vector (Promega, Madison, WI) and 5 μg of antioxidant response element–luciferase plasmid using iN-fect transfection reagent (iNtRON Biotechnology, Seongnam, Korea), according to the manufacturer's instructions. After 24 hours of transfection, the cells were treated with TGN for an additional 24 hours. The luciferase activity was determined using a dual luciferase assay system (Promega).

Trypan blue exclusion assay

For the trypan blue exclusion test, 5×10^4 cells per well were seeded in 12-well plates. After TGN treatment for 24 hours and 48 hours, cells were trypsinized and resuspended in 1 ml culture media. Next, 10 μl trypan blue (0.4%, Sigma-Aldrich) was added to 10 μl of cell suspension and 10 μl of the mixture was loaded in a hemocytometer. Only viable (non-stained) cells were counted.

Flow cytometric analysis of cell cycle

Cells were collected and fixed with cold 70% ethanol by adding drop-wise during shaking, and then incubated at −20°C. Ethanol was then removed and pellets were resuspended in staining solution containing 2 μg/ml propidium iodide, followed by a further incubation for 15 minutes at 37°C, protected from light. Cell cycles were analyzed using Fortessa flow cytometer (BD Biosciences, San Jose, CA).

Transient transfection of small interfering RNA

Cells that were about 80% confluent in 6-well plates were transfected with 100 nM scrambled, small interfering RNA,

NRF2 and HO-1 small interfering RNA (Bioneer, Daejeon, Korea) using Lipofectamine RNAiMAX (Invitrogen) for 48 hours before treatment. Cells were treated with cytokines and TGN and then used for subsequent experiments.

Chromatin immunoprecipitation

Chromatin immunoprecipitation was performed as previously described (Hiebert et al., 2018). Briefly, primary cultured murine keratinocytes were grown to 80−90% confluency in 14-cm culture dishes. Cells were treated with 10 μM TGN or DMSO as a control for 6 hours. Chromatin lysate was prepared by the homogenization of the cross-linked cell lysate. The chromatin and antibody-bead complexes were then subjected to immunoprecipitation. The following antibodies were used: anti-histone H3 (Abcam, Cambridge, United Kingdom), anti-NRF2 (Santa Cruz Biotechnology, Dallas, TX), and anti-rabbit IgG (Millipore, Burlington, MA). The samples were then captured using a magnetic tube rack (DynaMag-2 magnet, Thermo Fisher Scientific) and resuspended in a DNA elution buffer. The protein-DNA cross-links were reversed and the DNA was purified. DNA was then analyzed by real-time PCR for the presence of DNA fragments containing antioxidant response element promoter regions of *Ho1* and *Nqo1* using primers. The following primers were used: *Ho1* antioxidant response element, 5′-GGGGCTAGCATGCGAAGTGAG-3′ (F) and 5′-CAGGTCT GACTTGGGAATCCC-3′ (R); *Nqo1* antioxidant response element, 5′-AGCAGAACGCAGCACGAAT-3′ (F) and 5′-CACTCAGCCGTGGGAAGT-3′ (R).

Scoring severity of skin inflammation

Thickness, erythema, and scaling of back skin and ear were measured every other day throughout the entire 14 days of the experiment. The severity of the disease was measured using a semiquantitative scoring system. Erythema, scaling, and thickening of the skin were scored independently from 0 to 4 based on the macroscopic physical appearance of the mice: 0, none; 1, slight; 2, moderate; 3, marked; and 4, severe. Ear skin thickening was assessed by measuring thickness using an electronic digital caliper (Mitutoyo, Japan). The cumulative score (erythema plus scaling plus thickening) served as a measure of the severity of inflammation (scale 0−12).

Histology and immunohistochemistry

After a total of 14 days, all mice were euthanized and skin tissues were freshly harvested and fixed in 4% paraformaldehyde for histological and biochemical analysis. Skin tissues were embedded in paraffin, and the paraffin sections (3 μm) were stained with hematoxylin and eosin or incubated with antibodies against Ki-67, NF-κB p65, and p-STAT3 (1:200 dilution). Images were taken using a microscope IX70 (Olympus, Tokyo, Japan).

SUPPLEMENTARY REFERENCES

Hiebert P, Wietecha MS, Cangkrama M, Haertel E, Mavrogonatou E, Stumpe M, et al. Nrf2-mediated fibroblast reprogramming drives cellular senescence by targeting the matrisome. Dev Cell 2018;46:145−61.e10.

Lee J, Song K, Huh E, Oh MS, Kim YS. Neuroprotection against 6-OHDA toxicity in PC12 cells and mice through the Nrf2 pathway by a sesquiterpenoid from Tussilago farfara. Redox Biol 2018;18:6−15.

Park HR, Yoo MY, Seo JH, Kim IS, Kim NY, Kang JY, et al. Sesquiterpenoids isolated from the flower buds of Tussilago farfara L. inhibit diacylglycerol acyltransferase. J Agric Food Chem 2008;56:10493−7.

Siegenthaler B, Defila C, Muzumdar S, Beer HD, Meyer M, Tanner S, et al. Nrf3 promotes UV-induced keratinocyte apoptosis through suppression of cell adhesion. Cell Death Differ 2018;25:1749−65.

Song K, Lee KJ, Kim YS. Development of an efficient fractionation method for the preparative separation of sesquiterpenoids from Tussilago farfara by counter-current chromatography. J Chromatogr A 2017;1489:107−14.

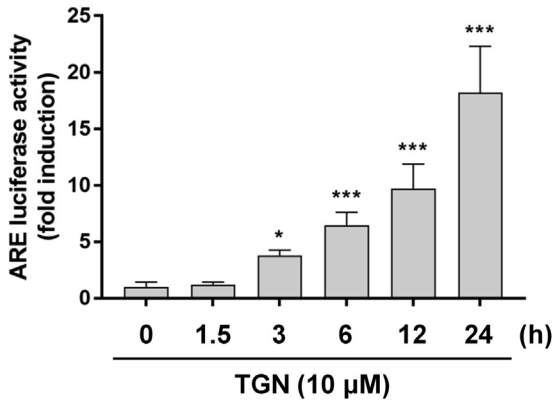

Supplementary Figure S1. Effect of TGN on the activation of ARE luciferase activity. HaCaT cells were treated with the indicated times of TGN. ARE-luciferase activity was measured using a dual luciferase assay (n = 4). $*P < 0.05$ and $***P < 0.001$ versus control. ARE, antioxidant response element; TGN, tussilagonone.

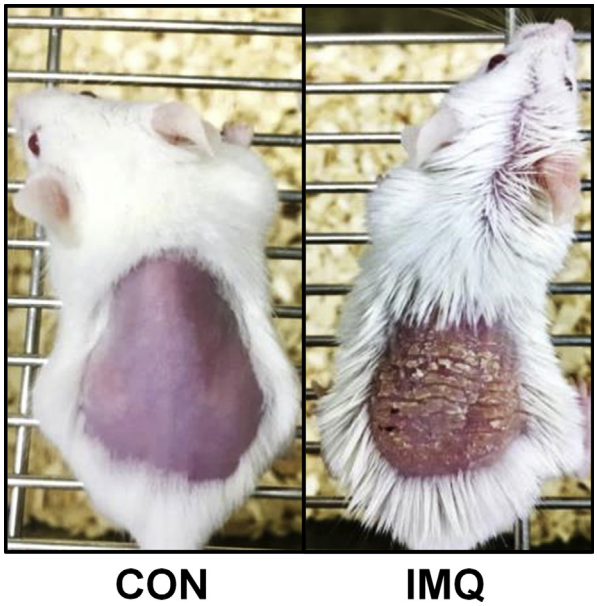

Supplementary Figure S2. Macroscopic appearance IMQ-treated mouse back skin. Photograph of mouse back skin was taken on the 5th day after IMQ treatment. CON, control; IMQ, imiquimod.

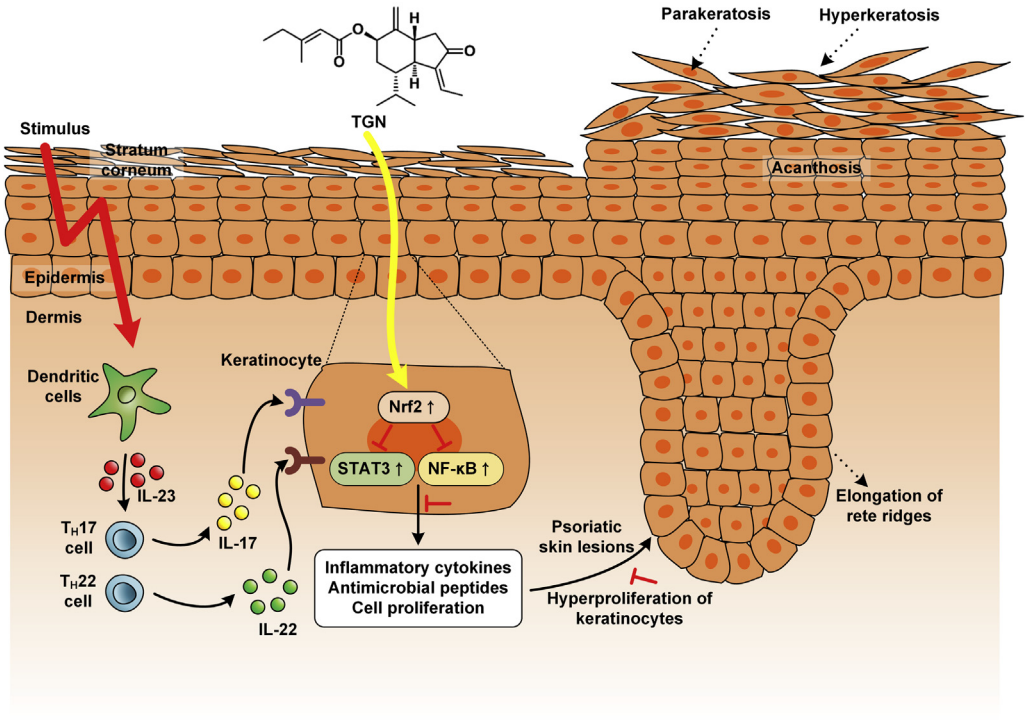

Supplementary Figure S3. The proposed mechanism of NRF2-mediated antipsoriatic effects of TGN by suppressing NF-κB and STAT3. TGN, tussilagonone; Th17, T helper type 17; Th22, T helper type 22.

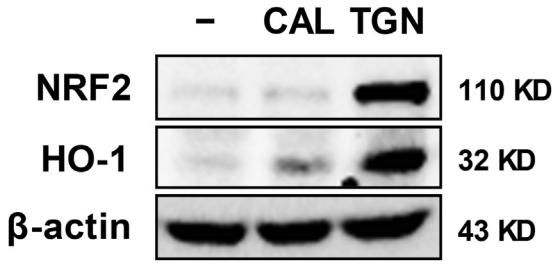

Supplementary Figure S4. Effect of CAL on the activation of NRF2/HO-1. HaCaT cells were treated with 10 nM CAL or 10 μM TGN for 6 hours. Protein levels of NRF2 and HO-1 were determined by western blotting. CAL, calcipotriol; TGN, tussilagonone.